# High-Resolution X-ray Diffraction and *ab Initio* Quantum Chemical Studies of Glycoluril, a Biotin Analog

**Naiyin Li,[1] Sergio Maluendes,[2,3] Robert H. Blessing,[1] Michel Dupuis,[2] Grant R. Moss,[1,4] and George T. DeTitta*,[1]**

*Contribution from the Medical Foundation of Buffalo, Inc., 73 High Street, Buffalo, New York 14203, and IBM, Neighborhood Road, Kingston, New York 12401*

*Received June 28, 1993®*

**Abstract:** The electrostatic properties of glycoluril, a model for the ureido ring of biotin, have been examined by high-resolution single-crystal X-ray diffraction and by *ab initio* quantum chemical calculation. Two crystalline forms of glycoluril were studied crystallographically, both at 105 K and at 293 K. Calculations were performed both on the isolated molecule and on a five-molecule cluster lifted out of one of the crystal structures. Qualitative agreement among the experiments and calculations was universal; quantitative agreement was observed between the low temperature diffraction results and the cluster calculations. The inner pocket of the bicyclic ring compound is a basin of negative electrostatic potential, reaching a minimum near the ureido oxygen atoms of –0.2 e/Å, while the back side of the molecule is everywhere of positive potential. The transferability of molecular properties from crystal form to crystal form extends beyond the electrostatic properties to include the rigid body thermal motions at a specific temperature. Anharmonic thermal motions of the oxygen and nitrogen atoms of glycoluril parallel nonrigid librations needed to model those same atoms in a rigid body formalism.

## Introduction

Glycoluril (**1**) is a bicyclic, *cis*-fused ring compound,[5] each ring of which resembles chemically the ureido ring of the vitamin biotin (**2**). All of the chemistry of biotin is thought to occur on the ureido ring, specifically at the $N_{1'}$ nitrogen atom.[6] The

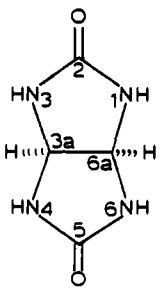


(1)

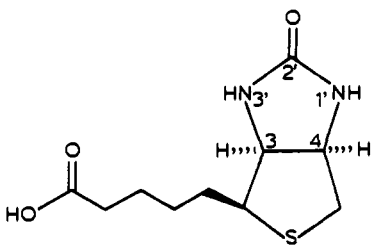


(2)

pentanoic acid side chain acts as an inert linking agent to the enzymes which biotin serves,[7] while the tetrahydrothiophene ring acts to maintain the planarity of the ureido ring,[8] to perhaps position the ureido ring properly at the active sites of catalysis,[9] and possibly to differentiate, via the electrostatic properties of the sulfur atom, the front and back sides of the ureido ring. There is evidence that the tetrahydrothiophene ring of biotin does not directly affect the chemistry of the ureido ring,[10,11] either by through-bond or through-space interactions. Therefore, we have undertaken a study of glycoluril as a model in duplicate of the chemically reactive moiety of the native coenzyme.

Glycoluril has been investigated by high-resolution X-ray diffraction and *ab initio* theoretical methods. Both techniques allow a mapping of the electrostatic properties of the ureido functionality. In our crystallographic studies two polymorphic forms of glycoluril were investigated, each form at two temperatures. In our *ab initio* quantum chemical studies, calculations on an isolated molecule and on a fragment of the higher symmetry crystal structure were undertaken. A consensus picture of the electronic properties of the ureido ring emerges when the results of the low temperature diffraction studies are compared with the *ab initio* calculations in the crystal structure fragment.

## Experimental Section and Results

**Preliminary Crystallographic Studies.** Glycoluril was crystallized from water. In the first crystallizations of commercial material it was apparent that two distinct forms crystallized simultaneously. X-ray diffraction photographs revealed that both polymorphs are orthorhombic. Crystals approximately square in cross section and pyramidally capped are in space group *Cmcm* (form A), while elongated, irregularly-hexagonal-in-cross-section crystals are in space group *Pnma* (form B). In subsequent crystallizations both forms appeared with quite similar habit and it was impossible to distinguish them by casual inspection alone. Powder diffraction analysis of the commercial product (Aldrich Chemical Co.) revealed the presence of form A only. As time went by it became increasingly difficult to secure crystals of form B, even when solutions near saturation were seeded with finely powdered material from prior crystallizations. Approximate unit cell dimensions for both forms were secured from the X-ray photographs. Observed densities, measured by flotation in $CCl_4$/$CH_2I_2$ mixtures, are quite high, 1.603 mg·mm$^{-3}$ for form A and 1.557 mg·mm$^{-3}$ for form B, suggesting (along with the approximate cell dimensions and space groups) that in form A the full molecular point group symmetry (*mm*2 or $C_{2v}$) was realized

* To whom correspondence may be addressed.

® Abstract published in *Advance ACS Abstracts,* June 15, 1994.

(1) Medical Foundation of Buffalo, Inc., 73 High St., Buffalo, NY 14203-1196.

(2) IBM, Neighborhood Rd., Kingston, NY 12401.

(3) Present address: Molecular Research Institute, Palo Alto, CA.

(4) Present address: BHP Petroleum, 120 Collins St., Melbourne, Australia.

(5) The systematic name of glycoluril is tetrahydroimidazo[4,5-*d*]imidazole-2,5(1*H*,3*H*)-dione.

(6) Knowles, J. *Annu. Rev. Biochem.* **1989**, *58*, 195–221.

(7) Kosow, D. P.; Lane, M. D. *Biochem. Biophys. Res. Commun.* **1962**, *7*, 439–443.

(8) DeTitta, G. T.; Edmonds, J. W.; Stallings, W.; Donohue, J. *J. Am. Chem. Soc.* **1976**, *98*, 1920–1926. Chen, C.-S.; Parthasarathy, R.; DeTitta, G. T. *J. Am. Chem. Soc.* **1976**, *98*, 4983–4990.

(9) DeTitta, G. T.; Parthasarathy, R.; Blessing, R. H.; Stallings, W. *Proc. Natl. Acad. Sci. U.S.A.* **1980**, *77*, 333–337.

(10) Berkessel, A.; Berslow, R. *Bioorg. Chem.* **1986**, *14*, 249–261.

(11) DeTitta, G. T.; Blessing, R. H.; Moss, G. R.; King, H. F.; Sukumaran, D. K.; Roskwitalski, R. L. *J. Am. Chem. Soc.*, preceding paper in this issue.

0002-7863/94/1516-6494$04.50/0 

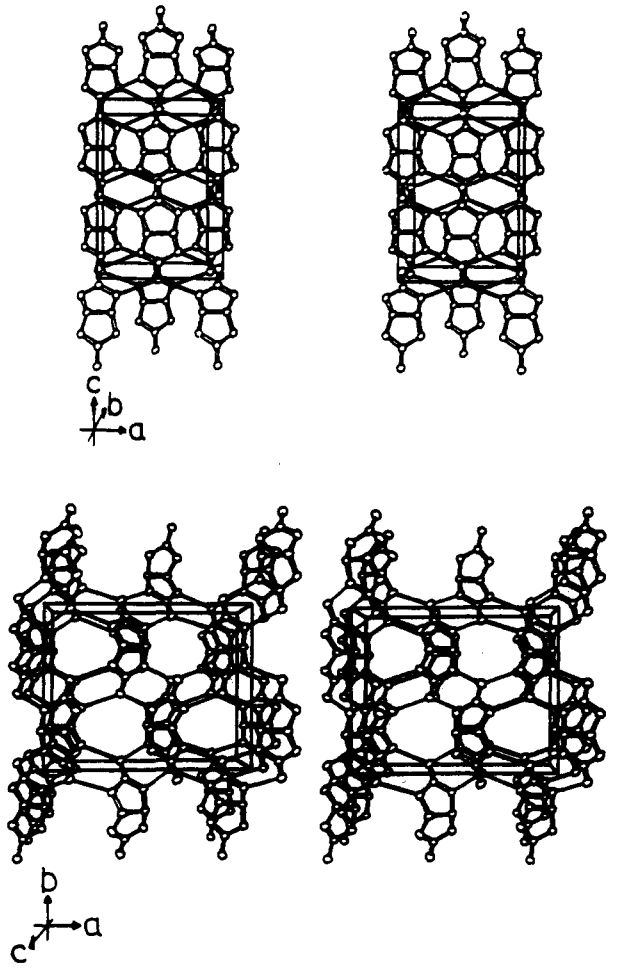


**Figure 1.** Crystal structures of glycoluril. Form A (top) is in space group *Cmcm*. Layers of hydrogen-bonded sheets of molecules stack in the *b*-axis direction. Form B (bottom) is in space group *Pnma*. There are three-dimensional ribbons of hydrogen-bonded molecules intersecting to link the crystal together.

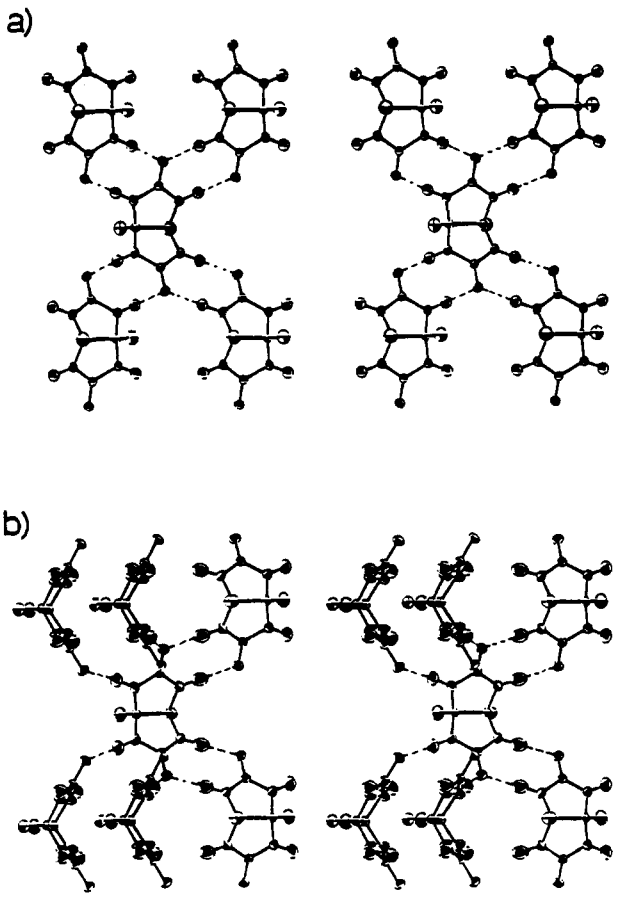


**Figure 2.** Stereoviews of the crystalline environment of a central glycoluril molecule in the two crystal forms. Shown are all hydrogen bonds made to and from the central molecule in the crystal lattices. In form A (a) the pentamer of molecules is mirror symmetric about a plane normal to the bridgehead C–C bond direction of the central molecule. Hydrogen-bonding rings are formed between pairs of molecules, all of the type $\overline{O_a{=}C_a{-}N_a{-}H_a{\cdots}O_b{=}C_b{-}N_b{-}H_b}$. Each carbonyl oxygen atom receives two hydrogen bonds along directions associated with the location of its lone pairs of electrons. In form B (b) the hydrogen bonding is more complex and less symmetric. The pattern to the right of the central molecule (as shown in figure) is very similar to that found in form A while on the left the situation is more complex. Ribbons of molecules come out of and go into the plane of the paper. While the carbonyl oxygen atom receives two hydrogen bonds again, the second comes from a molecule above the plane of the central molecule. The right side of the central molecule is described in the text as the "symmetric" side while the left side is termed the "dissymmetric" side. The hydrogen bonding on the dissymmetric side is of the type $\cdots O_a{=}C_a{-}N_a{-}H_a{\cdots}O_b{=}C_b{-}N_b{-}H_b{\cdots}O_c{=}C_c{-}N_c{-}H_c\cdots$.

crystallographically while in form B either one or the other (but not both) of the molecular mirror planes was realized crystallographically.

The crystal structures of both forms were determined in preliminary, low-resolution Cu K$\alpha$ experiments (not reported), the structure of form A by model-building techniques and that of form B by direct methods. They are shown in Figure 1.

In form A there are two-dimensional nets of molecules which are held together by hydrogen bonding. With respect to its four nearest neighbors in a net, a central fifth molecule is rotated 180° about its major inertial axis and positioned so that rings of hydrogen bonds are coplanar with the ureido rings forming them, Figure 2a. Thus, when viewed end-on, the sheets resemble herringbone, pleated sheets. The stacking of the sheets along the *b*-axis is of type ABABA..., with the hills in one sheet fitting the valleys of the sheet above. There are no hydrogen bonds connecting sheets, and the molecules in one sheet minimally overlap those in the sheets immediately above and below, except that the carbonyl C=O bonds form an antiparallel stepladder running the entire *b* direction in the crystal. The rungs of the ladder are inclined ~60° with respect to *b*, with C···O nonbonded separation of 2.73 Å. All of the potential H-bond donors are involved in hydrogen bonding, with the carbonyl oxygen atoms each accepting two hydrogen bonds, each in the plane of their ureido rings and each approximately along directions associated with lone pairs of electrons on the oxygen atoms.

In form B the hydrogen bonding is three-dimensional. The molecular mirror plane taking one ureido ring of the molecule into the other ring is expressed crystallographically, while the molecular bilateral symmetry (e.g., relating a nitrogen atom of one ring to the other nitrogen atom of the *same* ring) is broken by the crystalline environment, Figure 2b. In form B the hydrogen-bonding network on the symmetric side of the molecule (involving both rings of one molecule) looks like that observed on *both* sides of the molecule in form A, while on the dissymmetric side of the molecule the acceptor of an NH···O hydrogen bond is not the same molecule as the donor in the O···HN hydrogen bond.

**Room Temperature High Resolution Diffraction Experiments.** Approximately equidimensional crystals of both form A and form B were employed in the room temperature diffraction experiments. Their mean diameters were approximately 0.25 mm. The room temperature was ~293 K with a variation of less than ±2 K. Intensity data were recorded as $\theta/2\theta$ scans employing Mo K$\bar{\alpha}$ radiation (50 kV) with niobium filtering. Data in the form of scan profiles (counts versus $\theta$) were recorded to $\sin\theta_{max}/\lambda = 1.30$

Table 1. Crystal Data for Glycoluril ($C_4H_6N_4O_2$) at 293 and 105 K

| | form A | | form B | |
|---|---|---|---|---|
| | 293 K | 105 K | 293 K | 105 K |
| space group | *Cmcm* (No. 63) | | *Pnma* (No. 62) | |
| no. of molecules cell | 4 | | 4 | |
| cell dimens | | | | |
| *a*, Å | 7.3768(9) | 7.375(1) | 12.591(3) | 12.515(2) |
| *b*, Å | 7.538(1) | 7.373(2) | 10.158(3) | 10.102(2) |
| *c*, Å | 10.578(1) | 10.567(1) | 4.748(1) | 4.715(2) |
| vol, Å$^3$ | 588.23(23) | 574.62(18) | 607.30(47) | 596.08(25) |
| density (calcd), g/cm$^3$ | 1.605 | 1.643 | 1.554 | 1.584 |

Å$^{-1}$ for form A and 1.19 Å$^{-1}$ for form B. For each form ~13 000 reflections were measured over an ~800-h period. This represented a >4-fold redundancy for form A and about a 3-fold redundancy for form B. The scan profile data were corrected for background subtraction and Lorentz, polarization, and time-dependent scaling effects using procedures[12] developed by one of us. Time-dependent scaling factors determined from fits to various standard reflections scattered both high and low in reciprocal space showed an ~3% decrease in intensity for the form A crystal and an ~15% decrease for the form B crystal over the course of the experiments. Agreement indices for averaging replicate and/or space group equivalent reflections were $R_{sym} = \sum|F_i^2 - \overline{F^2}|/\sum|F_i^2| = 0.015$ for form A and $R_{sym} = 0.018$ for form B based on $F^2$. Replicate data were sorted and merged to give 2868 unique reflections for form A and 4337 unique reflections for form B, of which 1117 and 1747 had $I > 2\sigma_I$, respectively.

**Low-Temperature High Resolution Diffraction Experiments.** Experiments were carried out as in the room temperature case, except that crystals were cooled to approximately 105 K using a nitrogen gas cold stream device.[13] Diffraction data at 105 K were recorded for both form A and form B employing approximately equidimensional crystals (maximum dimension 0.7 mm). Diffraction data from two separate crystals were recorded for each form to 1.2-Å$^{-1}$ resolution with a minimum of 8-fold redundancy. In the experiment on the second crystal of form B, high-resolution data ($\sin\theta/\lambda \geq 0.9$ Å$^{-1}$) for which $I/\sigma_I$ exceeded 3.0 in the experiment on the first crystal were remeasured, while all of the data for which $\sin\theta/\lambda < 0.9$ Å$^{-1}$ were remeasured regardless of the $I/\sigma_I$ ratio. Approximately 24 000 measurements were recorded for each of the forms, each over an ~700-h period. Time-dependent variation in the intensity of standard reflections was about 4% for form A and 1% for form B. Agreement indices for the averaging of replicate measurements were $R_{sym} = 0.018$ for form A and $R_{sym} = 0.014$ for form B. There were, after averaging, 2146 unique reflections for form A, of which 1901 had $I > 2\sigma_I$, and 3232 unique reflections for form B, of which 2736 had $I > 2\sigma_I$.

**Lattice Parameter Measurements.** At both temperatures lattice parameters were determined by least-squares fitting to the centered $2\theta$ positions of reflection profiles. At room temperature, 24 reflections with $2\theta \approx 32°$ were employed and an effective Mo K$\bar{\alpha}$ wavelength of $(2\lambda_{MoK\alpha_1} + 1\lambda_{MoK\alpha_2})/3 = 0.7107$ Å was assumed, since the $\alpha_1$, $\alpha_2$ doublet was not cleanly resolved ($\Delta 2\theta \approx 0.2°$). However, at low temperature it proved possible to accurately center reflections with $2\theta > 95°$ and there the $\alpha_1$ peak (used for centering) was cleanly resolved from the $\alpha_2$ peak, suggesting that a wavelength of 0.7093 Å was appropriate for the refinement of lattice parameters. The results of the refinements are summarized in Table 1.

**Charge Density Refinement Model.** The diffraction results were modeled in the rigid pseudoatom approximation using MOLLY.[14] MOLLY is a crystallographic refinement program that allows adjustment of both standard crystallographic parameters, such as the scale factor, an extinction model, atomic positional and occupancy parameters, and harmonic, anisotropic atomic displacement parameters, or ADPs, and the adjustment of additional parameters that allow for anharmonic, anisotropic ADPs in a Gram–Charlier expansion about the harmonic ADPs and for departures from atomic spherical symmetry in the rigid pseudoatom approximation. For the latter, the atomic density is modeled on atom $j$ as

$$\rho_j(\vec{r}) = P_{j,\text{core}}\,\rho_{j,\text{core}}(|r|) + P_{j,\text{valence}}\kappa'^3\rho_{j,\text{valence}}(\kappa' r) + \sum_{l=0}^{L}\sum_{m=-l}^{l} P_{j,l,m}\kappa''^3 R_{j,l}(\kappa'' r)\, Y_{j,l,m}(\theta_j,\phi_j)$$

The first term on the right-hand side involves the unperturbed core density $\rho_{j,\text{core}}$, nominally the $1s^2$ shell for first-row atoms other than hydrogen, and an occupancy parameter $P_{j,\text{core}}$ that is usually fixed by the crystallographic site occupancy of the atom. The second term involves a spherical, perturbed, valence shell density $\rho_{j,\text{valence}}$. For $\kappa' > 1$ the valence shell is "contracted", that is, the valence density at $|r|$ is equal to the isolated atom valence density at a point more distant from the nucleus. The electron population for the valence shell of atom $j$ is given by $P_{j,\text{valence}}$. The term $\kappa'^3$ is a normalization factor that allows the model to adjust electron *density* (e/Å$^3$) while maintaining a fixed *number* of electrons (usually normalized to 1). The third term allows for a redistribution of the valence shell density to take account of the nonspherical effects of bonding. The terms $Y_{j,l,m}$ are a finite set of harmonic functions mapped on a sphere of unit radius. The angles $\theta_j$ and $\phi_j$ are specified in a local axial frame with the nucleus of atom $j$ as origin. The orthonormal frame can be fixed by the unit cell directions (which aids in specifying crystallographic symmetry requirements on the $P_{j,l,m}$ terms for atoms at site symmetries other than 1) or along directions of particular interest in the molecule. For each value of $l$ all permissible values of $m$ ($-l \leq m \leq +l$) must be included in the model for completeness of the expansion at the level specified by $l$ ($l = 0$, monopole; $l = 1$, dipole; $l = 2$, quadrupole; $l = 3$, octapole; $l = 4$, hexadecapole); this assures rotational invariance.[15] The term $R_{j,l}$ governs the

$$R_{j,l}(\kappa'' r) = \frac{\alpha_j^{\,n_l+3}}{(n_l+2)!}\kappa''^3 r^{n_l} e^{-\alpha_j r\kappa''}$$

radial dependence of the nonspherical redistribution of density. Here, $\alpha_j$ is taken as $2\zeta_j$ where $\zeta_j$ is the average Slater screening constant[16] for the ground state of the neutral atom, $\kappa''$ acts again to contract or expand the deformation functions as it is greater than or less than 1, respectively, $(\kappa'')^3$ appears as a normalization parameter, and the values $n_l$ are chosen such that $n_l \geq l$ in order to satisfy the Poisson condition. $P_{j,l,m}$ is an occupany parameter that is refined.

It should be appreciated that the model is very flexible; therefore it was limited in the following ways. The monopole population ($l = 0$; $P_{j,0,0}$) parameters, unlike the higher multipole terms, add or subtract, as opposed to merely rearrange, electron density associated with the atom, and thus they are likely to correlate strongly with the $P_{j,\text{valence}}$ values. They were, therefore, not refined. For non-hydrogen atoms, values $n_l = \{2,2,3,4\}$ corresponding to $l = 1$–4 were adopted; these values were not optimized. Hydrogen atoms, which have no core electrons, were allowed dipole ($l = 1$) and quadrupole ($l = 2$) deformation terms, but these were constrained to have cylindrical symmetry along the C–H or N–H

(12) Blessing, R. H. *Cryst. Rev.* **1987**, *1*, 3–58.
(13) DeTitta, G. T. ACA Workshop on Accurate Single-Crystal Diffractometry 1990, American Crystallographic Assoc. Meeting, April 1990, New Orleans, LA. Additional details deposited.
(14) Hansen, N. K.; Coppens, P. *Acta Crystallogr.* **1978**, *A34*, 909–921. Coppens, P.; Hansen, N. K. *Isr. J. Chem.* **1977**, *16*, 163–167.
(15) Kurki-Suonio, K. *Isr. J. Chem.* **1977**, *16*, 115–123.
(16) Clementi, E.; Raimondi, D. L. *J. Chem. Phys.* **1963**, *38*, 2686–2689.

**Table 2.** $\kappa$ Values[a] and $\zeta$ Values

| | $\kappa'$ | $\kappa''$ | $\zeta$ |
|---|---|---|---|
| O(2) | 0.985 692 | 0.713 667 | 4.472 |
| N(1),N(3) | 0.995 655 | 0.960 815 | 3.841 |
| C(2) | 0.985 226 | 0.909 522 | 3.176 |
| C(6a),C(3a) | 0.985 883 | 0.897 370 | 3.176 |
| H(1),H(3) | 1.079 365 | 1.079 365 | 2.000 |
| H(6a),H(3a) | 1.066 142 | 1.066 142 | 2.000 |

[a] The $\kappa$ values are calculated by averaging the refined $\kappa$ values from 105 K multipole refinement of glycoluril form A, form B, and 95 K d(+)biotin.[17]

**Table 3.** Refinement Details[a]

| | $R(F)$ | $R_w(F)$ | $N_o$ | $N_v$ | GOF | $K$ |
|---|---|---|---|---|---|---|
| a. Low-Temperature Data Multipole Refinement Results | | | | | | |
| form A | 0.0143 | 0.0102 | 2089 | 103[b] | 0.83 | 2.251(1) |
| form B | 0.0238 | 0.0110 | 3138 | 189[b] | 0.72 | 0.9197(4) |
| b. Room Temperature Pseudomultipole Refinement | | | | | | |
| form A | 0.106 | 0.031 | 2868 | 44[c] | 1.12 | 0.890(1) |
| form B | 0.105 | 0.034 | 4337 | 79[c] | 1.17 | 1.043(1) |
| c. Room Temperature Multipole Refinement[d] | | | | | | |
| form A | 0.105 | 0.030 | 2868 | 103 | 1.10 | 0.888(1) |
| form B | 0.103 | 0.032 | 4337 | 189 | 1.23 | 1.041(1) |

[a] $R(F) = \sum|\Delta|/\sum|F_o|$. $R_w(F) = [\chi^2/\sum w|F_o|^2]^{1/2}$. GOF $= [\chi^2/(N_o - N_v)]^{1/2}$. $\Delta = |F_o| - K^{-1}|F_c|$. $\chi^2 = \sum w\Delta^2$. $w = 1/\sigma^2(|F_o|)$. $K$: scale factor. $N_o$: number of observations. $N_v$: number of refined variables. $F_o$: observed structure factor. $F_c$: calculated structure factor. [b] Refine $x_l'$, $U_{jk}$, for non-H atoms. Refine $C_{ijk}$ for O(2), N(1), and N(3) atoms. $\kappa$ values are fixed at the average value based on 105 K glycoluril and 95 K biotin refinements. Multipole parameters up to $l = 3$ for O(2), C(2), N(1), and N(3) atoms, $l = 4$ for C(6a) and C(3a) atoms, and $l = 2$ with cylindrical symmetry for all H atoms. [c] Multipole parameters are fixed at the low-temperature refinement results. $x_l'$, $U^{jk}$ are refined for non-H atoms, $C_{ijk}$ are refined for O(2), N(1), and N(3) atoms. [d] The same parameters were refined as in part a.

bond. Although the positions of the hydrogen atoms were allowed to vary, just prior to the final cycle of least squares, the C–H hydrogen positions were reset along the C→H vectors to standard bond lengths of 1.090 Å and the N–H hydrogens were likewise repositioned with standard N–H bond lengths of 1.004 Å. Values of $n_l$ for hydrogen atoms were $n_l = 1$ for $l = 1$ (dipole) and $n_l = 2$ for $l = 2$ (quadrupole). Values of $\kappa'$ and $\kappa''$ were allowed to vary for all atoms in both forms in the initial low-temperature refinements. From the penultimate cycles of the 105 K refinements, consensus values of $\kappa'$ and $\kappa''$ for each chemically equivalent atom were calculated from the average values across the two forms, along with the values from a recent high-resolution investigation of *d*-biotin.[17] In the final cycles these consensus $\kappa'$ and $\kappa''$ values were fixed. Likewise, these $\kappa$ values were assumed for the room temperature refinements (although refined values did not differ significantly); thus all of the maps shown are referred to the same set of $\kappa$ values, Table 2. A common coordinate frame was used to specify the $\{\theta_j,\phi_j\}$ values in all refinements so, in principle, values of $P_{j,l,m}$ should be directly comparable. Although the molecular point group is higher than the crystallographic site symmetry for glycoluril in form B, no noncrystallographic symmetry was imposed upon the model apart from that discussed for the hydrogen atoms. Thus departures from *mm*2 ($C_{2v}$) symmetry in the electron density maps due to a nonsymmetric crystal environment could be accounted in the least-squares model if they were present.

Agreement in refinements was based on minimizing the weighted sum $\sum w_i(|F_o| - K^{-1}|F_c|)^2$, where $K$ is a scale factor, $w_i = 1/\sigma_i^2$, and $\sigma_i$ is from a complete analysis of variance in the data processing programs.[12] Results of refinements of the following parameters are reported: a single scale factor, positional parameters for all non-hydrogen atoms, valence occupancy parameters, $P_{j,\text{valence}}$ and anisotropic, harmonic ADPs for all atoms, third cumulant anharmonic ADPs for the oxygen and nitrogen atoms, multipole function occupancies $P_{j,l,m}$ up to $l = 3$ for oxygen, nitrogen, and carbonyl carbon atoms, and up to $l = 4$ for the bridgehead carbon atoms. The treatment of the hydrogen atoms and the $\kappa$ values has already been described (*vide supra*). Final agreement indices for the refinements are collected in Table 3, final positional and atomic displacement parameters in Table 4, and final multipole function occupancies in Table 5. As a measure of the completeness of the refinements, residual density maps calculated as $\Delta F = F_{obs} - F_{multipole}$ in the principal plane of the rings are featureless and have been deposited.

(17) Li, N.; DeTitta, G. T. *J. Am. Chem. Soc.*, in preparation.

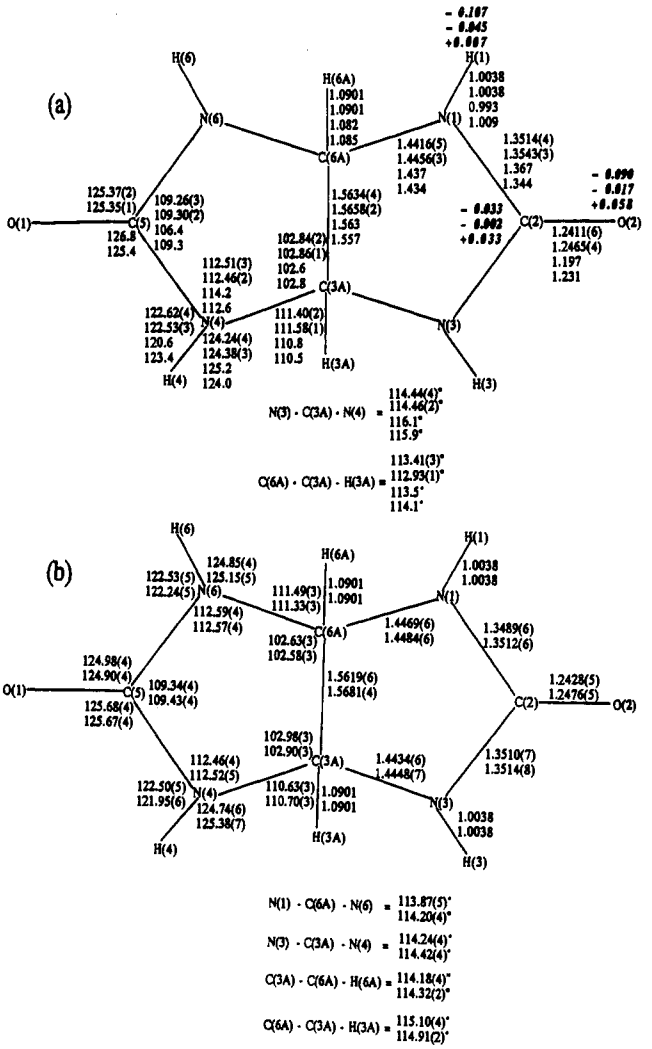


**Figure 3.** Bond distances, angles, and deviations from planes for glycoluril from multipole refinements and quantum calculations. (a) Form A at 105 K, form A at 293 K, monomer, central molecule of pentamer, from top to bottom. Values in bold italcs are deviations from least-squares planes fitted to bond-contiguous atoms N–C–C–N and are for form A at 105 K, the central molecule of the pentamer, and isolated monomer, from top to bottom. (b) Form B at 105 K and at 293 K. In form A, the monomer, and the central molecule of the pentamer, the molecular symmetry is *mm*2 ($C_{2v}$); in form B, the mirror plane relating one ureido ring to the other (left to right in drawing) is expressed crystallographically while the molecular mirror plane bisecting and perpendicular to the bridgehead C–C bond is broken by the crystalline environment.

**Geometry of the Molecule from the Diffraction Studies.** The glycoluril molecule is shaped like a butterfly, with the rings, as wings, *cis*-fused as they are in biotin. Bond distances and angles are shown in Figure 3 for both forms at both temperatures. The ureido functionality, as evidenced by its geometry, presents a consistent picture across crystal environment and temperature, allowing a consensus description in terms of an average C=O

**Table 4.** Positional and Displacement Parameters for Glycoluril

a. Fractional Atomic Coordinates from 105 K (Top Line) and 293 K (Bottom Line) Multipole Refinements[a]

| atoms | x/a | y/b | z/c | atoms | x/a | y/b | z/c |
|---|---|---|---|---|---|---|---|
| form A | | | | | | | |
| O(2) | 0 | 0.776 68(5) | 0.534 88(3) | C(6a) | 0.106 16(2) | 0.551 30(2) | 0.25 |
| O(2) | 0 | 0.775 53(28) | 0.533 27(12) | C(6a) | 0.105 99(5) | 0.554 68(7) | 0.25 |
| N(1) | 0.149 78(4) | 0.648 04(5) | 0.365 03(3) | H(1) | 0.275 49 | 0.660 86 | 0.400 36 |
| N(1) | 0.149 05(15) | 0.649 25(29) | 0.364 41(1) | H(1) | 0.274 78 | 0.661 44 | 0.399 66 |
| C(2) | 0 | 0.697 95(2) | 0.430 49(1) | H(6a) | 0.163 74 | 0.415 13 | 0.25 |
| C(2) | 0 | 0.698 29(7) | 0.429 75(4) | H(6a) | 0.164 72 | 0.421 97 | 0.25 |
| form B | | | | | | | |
| O(2) | 0.631 12(3) | −0.041 90(4) | 0.326 35(10) | C(3a) | 0.616 31(2) | 0.25 | −0.082 38(6) |
| O(2) | 0.631 51(11) | −0.040 22(14) | 0.329 22(41) | C(3a) | 0.618 24(6) | 0.25 | −0.073 98(17) |
| N(1) | 0.513 44(5) | 0.129 61(6) | 0.246 87(15) | H(1) | 0.457 70 | 0.098 38 | 0.384 61 |
| N(1) | 0.515 65(16) | 0.130 99(20) | 0.249 24(58) | H(1) | 0.459 77 | 0.100 48 | 0.385 18 |
| N(3) | 0.666 72(6) | 0.129 77(7) | 0.015 81(18) | H(3) | 0.736 18 | 0.093 19 | −0.056 29 |
| N(3) | 0.667 56(22) | 0.131 25(25) | 0.024 25(74) | H(3) | 0.736 26 | 0.094 57 | −0.048 93 |
| C(2) | 0.606 15(1) | 0.063 74(2) | 0.206 33(4) | H(6a) | 0.436 94 | 0.25 | −0.056 01 |
| C(2) | 0.607 11(4) | 0.064 69(5) | 0.211 16(12) | H(6a) | 0.440 40 | 0.25 | −0.053 00 |
| C(6a) | 0.507 15(2) | 0.25 | 0.080 85(6) | H(3a) | 0.609 51 | 0.25 | −0.312 88 |
| C(6a) | 0.509 51(5) | 0.25 | 0.085 30(16) | H(3a) | 0.612 55 | 0.25 | −0.303 06 |

b. Anisotropic, Harmonic Mean-Square Displacement Parameters[b]

| | $U^{11}$ | $U^{22}$ | $U^{33}$ | $U^{12}$ | $U^{13}$ | $U^{23}$ |
|---|---|---|---|---|---|---|
| form A | | | | | | |
| O(2) | 0.009 38(3) | 0.023 33(5) | 0.010 24(3) | 0 | 0 | −0.005 38(3) |
| O(2) | 0.022 51(13) | 0.061 09(30) | 0.025 61(15) | 0 | 0 | −0.013 62(20) |
| N(1) | 0.006 94(2) | 0.025 25(4) | 0.010 37(2) | 0.000 50(2) | −0.000 28(2) | −0.005 01(2) |
| N(1) | 0.016 85(9) | 0.059 82(24) | 0.024 11(11) | 0.001 85(13) | −0.000 88(9) | −0.009 80(15) |
| C(2) | 0.007 56(3) | 0.016 08(4) | 0.008 12(3) | 0 | 0 | −0.001 40(3) |
| C(2) | 0.018 09(12) | 0.041 54(23) | 0.019 59(13) | 0 | 0 | −0.003 23(15) |
| C(6a) | 0.008 76(3) | 0.013 64(4) | 0.008 34(3) | 0.001 49(3) | 0 | 0 |
| C(6a) | 0.021 49(12) | 0.034 61(19) | 0.020 08(13) | 0.004 43(14) | 0 | 0 |
| H(1) | 0.012 98 | 0.028 09 | 0.014 80 | −0.000 15 | −0.000 05 | −0.003 46 |
| H(1) | 0.020 67 | 0.048 10 | 0.036 74 | −0.001 99 | −0.007 67 | −0.001 35 |
| H(6a) | 0.019 91 | 0.026 19 | 0.021 58 | 0.003 16 | 0 | 0 |
| H(6a) | 0.041 27 | 0.058 77 | 0.044 24 | 0.010 15 | 0 | 0 |
| form B | | | | | | |
| O(2) | 0.011 27(5) | 0.010 92(5) | 0.017 89(10) | 0.002 12(4) | 0.000 28(5) | 0.003 83(5) |
| O(2) | 0.028 44(17) | 0.028 11(19) | 0.046 84(41) | 0.005 21(16) | 0.001 36(18) | 0.009 75(21) |
| N(1) | 0.010 37(5) | 0.011 32(5) | 0.018 01(7) | 0.002 40(5) | 0.003 84(6) | 0.004 59(6) |
| N(1) | 0.024 92(19) | 0.026 58(20) | 0.043 75(20) | 0.004 50(18) | 0.007 55(22) | 0.008 76(23) |
| N(3) | 0.014 36(6) | 0.013 12(6) | 0.024 30(1) | 0.004 61(6) | 0.009 43(7) | 0.006 19(7) |
| N(3) | 0.034 30(26) | 0.030 20(25) | 0.053 35(39) | 0.008 93(23) | 0.018 93(29) | 0.010 70(30) |
| C(2) | 0.009 21(5) | 0.008 71(5) | 0.012 90(6) | 0.000 96(4) | 0.000 39(5) | 0.001 07(5) |
| C(2) | 0.023 37(16) | 0.021 96(16) | 0.032 86(21) | 0.002 31(15) | 0.000 28(16) | 0.002 01(17) |
| C(6a) | 0.009 39(7) | 0.008 41(7) | 0.012 36(8) | 0 | −0.001 17(7) | 0 |
| C(6a) | 0.023 54(23) | 0.020 46(23) | 0.031 76(28) | 0 | −0.003 86(23) | 0 |
| C(3a) | 0.013 05(8) | 0.009 57(7) | 0.010 28(8) | 0 | 0.001 48(7) | 0 |
| C(3a) | 0.034 72(31) | 0.023 58(26) | 0.025 24(28) | 0 | 0.003 62(25) | 0 |
| H(1) | 0.021 35 | 0.019 25 | 0.036 73 | 0.002 88 | −0.000 03 | 0.000 68 |
| H(1) | 0.023 73 | 0.038 53 | 0.064 55 | −0.005 06 | 0.004 71 | 0.004 43 |
| H(3) | 0.018 04 | 0.023 08 | 0.026 79 | 0.003 98 | 0.007 16 | 0.003 04 |
| H(3) | 0.032 95 | 0.042 49 | 0.051 03 | 0.007 03 | 0.016 15 | −0.005 04 |
| H(6a) | 0.019 27 | 0.017 86 | 0.021 70 | 0 | −0.005 12 | 0 |
| H(6a) | 0.046 57 | 0.042 30 | 0.056 12 | 0 | −0.019 83 | 0 |
| H(3a) | 0.023 52 | 0.025 32 | 0.014 37 | 0 | 0.000 50 | 0 |
| H(3a) | 0.045 10 | 0.059 48 | 0.036 51 | 0 | 0.015 14 | 0 |

c. Third-Order Anharmonic Parameters ($\times 10^3$) r

| | | form A | | form B | | | form A | | form B | |
|---|---|---|---|---|---|---|---|---|---|---|
| | | 293 K | 105 K | 293 K | 105 K | | 293 K | 105 K | 293 K | 105 K |
| O(2) | C111 | | | 0.10(12) | 0.01(3) | C113 | −0.08(4) | 0.027(7) | −0.24(7) | 0.01(2) |
| | C222 | 0.36(27) | 0.120(27) | 0.47(13) | 0.01(3) | C133 | | | 0.65(9) | 0.10(1) |
| | C333 | −0.44(10) | 0.008(14) | 0.39(22) | 0.15(4) | C223 | −0.66(10) | −0.062(11) | 0.63(8) | 0.11(2) |
| | C112 | −0.05(6) | 0.020(8) | 0.10(6) | −0.02(1) | C233 | 0.60(8) | 0.130(9) | 0.76(9) | 0.05(2) |
| | C122 | | | 0.22(6) | 0.03(1) | C123 | | | 0.20(5) | 0.06(1) |
| N(1) | C111 | −0.13(6) | −0.003(11) | 0.49(14) | 0.04(3) | C113 | −0.03(3) | −0.010(5) | 0.38(8) | 0.07(2) |
| | C222 | 0.09(24) | −0.060(24) | 0.29(15) | −0.11(3) | C133 | −0.15(4) | −0.030(5) | 0.42(10) | 0.12(2) |
| | C333 | −0.18(8) | −0.021(12) | −0.74(26) | 0.08(5) | C223 | 0.21(8) | 0.068(9) | 0.10(11) | 0.04(2) |
| | C112 | −0.18(5) | −0.015(7) | 0.24(7) | 0.01(2) | C233 | 0.09(6) | 0.020(7) | −0.08(6) | −0.03(2) |
| | C122 | −0.46(7) | −0.103(9) | 0.18(7) | 0.05(2) | C123 | 0.25(3) | 0.062(5) | 0.01(3) | 0.05(1) |
| N(3) | C111 | | | −0.78(21) | −0.11(4) | C113 | | | −0.45(14) | −0.12(3) |
| | C222 | | | 0.40(19) | −0.01(4) | C133 | | | −0.10(15) | −0.06(3) |
| | C333 | | | 0.15(35) | 0.01(6) | C223 | | | 0.49(12) | 0.10(2) |
| | C112 | | | 0.12(10) | −0.02(2) | C233 | | | 0.75(15) | 0.11(3) |
| | C122 | | | 0.25(9) | 0.06(2) | C123 | | | 0.03(8) | −0.02(2) |

[a] Hydrogen atoms are fixed at the neutron distances CH–N = 1.0039 Å, H–C = 1.0901 Å). [b] Temperature factors for hydrogen atoms were obtained from the penultimate cycles of refinement and then fixed for the final cycles of refinement at the neutron-predicted positions.

**Table 5.** Multipolar Coefficients of Each Atom[a] at 105 K

| atom | $P_{val}$ | $P_{11+}$ | $P_{11-}$ | $P_{10}$ | $P_{20}$ | $P_{21+}$ | $P_{21-}$ | $P_{22+}$ | $P_{22-}$ | $P_{30}$ | $P_{31+}$ |
|---|---|---|---|---|---|---|---|---|---|---|---|
| form A | | | | | | | | | | | |
| O(2) | 6.230(9) | 0.002(8) | | −0.120(9) | −0.092(6) | −0.013(6) | | −0.079(5) | | 0.033(6) | −0.001(7) |
| N(1) | 5.152(10) | −0.002(6) | −0.002(5) | 0.036(6) | 0.040(4) | −0.000(3) | −0.015(3) | 0.042(3) | −0.010(3) | 0.159(4) | −0.005(4) |
| C(2) | 4.216(16) | −0.004(6) | | 0.103(8) | 0.257(6) | −0.006(6) | | −0.196(6) | | 0.384(8) | −0.008(7) |
| C(6a) | 4.157(17) | | 0.064(9) | 0.012(7) | −0.004(5) | | −0.089(6) | −0.047(6) | | 0.270(8) | |
| H(1) | 0.669(6) | | | 0.147(7) | 0.051(9) | | | 0.014(7) | | | |
| H(6a) | 0.754(10) | | | 0.162(9) | 0.036(12) | | | 0.036(10) | | | |

| | $P_{31-}$ | $P_{32+}$ | $P_{32-}$ | $P_{33+}$ | $P_{33-}$ | $P_{40}$ | $P_{41-}$ | $P_{42+}$ | $P_{43-}$ | $P_{44+}$ |
|---|---|---|---|---|---|---|---|---|---|---|
| form A | | | | | | | | | | |
| O(2) | | 0.013(6) | | −0.003(5) | | | | | | |
| N(1) | 0.005(4) | 0.109(4) | −0.013(4) | 0.020(4) | −0.003(4) | | | | | |
| C(2) | | 0.248(8) | | 0.002(6) | | | | | | |
| C(6a) | 0.072(6) | 0.044(6) | | | 0.298(7) | 0.066(8) | −0.005(7) | −0.059(7) | −0.116(8) | −0.024(8) |

| atom | $P_{val}$ | $P_{11+}$ | $P_{11-}$ | $P_{10}$ | $P_{20}$ | $P_{21+}$ | $P_{21-}$ | $P_{22+}$ | $P_{22-}$ | $P_{30}$ | $P_{31+}$ |
|---|---|---|---|---|---|---|---|---|---|---|---|
| form B | | | | | | | | | | | |
| O(2) | 6.211(9) | 0.002(9) | −0.014(8) | −0.105(10) | −0.088(6) | 0.001(6) | −0.011(6) | −0.085(5) | −0.001(5) | 0.024(7) | −0.003(6) |
| N(1) | 5.128(13) | −0.005(9) | −0.027(8) | 0.010(10) | 0.044(6) | −0.005(4) | −0.006(5) | 0.048(5) | −0.000(5) | 0.162(6) | −0.004(5) |
| N(3) | 5.174(14) | −0.007(10) | −0.018(10) | 0.023(10) | 0.055(6) | 0.002(5) | −0.023(5) | 0.030(6) | 0.001(5) | 0.178(7) | −0.020(5) |
| C(2) | 4.236(14) | −0.005(6) | −0.007(7) | 0.101(8) | 0.265(7) | −0.003(6) | 0.005(7) | −0.207(6) | 0.000(5) | 0.378(8) | −0.013(7) |
| C(6a) | 4.167(22) | | 0.087(11) | −0.018(9) | 0.002(9) | | −0.087(8) | −0.074(8) | | 0.281(11) | |
| C(3a) | 4.180(24) | | 0.107(12) | −0.007(10) | −0.012(10) | | −0.085(9) | −0.078(8) | | 0.285(11) | |
| H(1) | 0.705(8) | | | 0.173(9) | 0.059(10) | | | −0.005(7) | | | |
| H(3) | 0.657(7) | | | 0.146(8) | 0.070(10) | | | −0.002(7) | | | |
| H(6a) | 0.715(13) | | | 0.125(11) | 0.028(12) | | | 0.014(12) | | | |
| H(3a) | 0.715(13) | | | 0.089(11) | 0.001(13) | | | −0.020(12) | | | |

| | $P_{31-}$ | $P_{32+}$ | $P_{32-}$ | $P_{33+}$ | $P_{33-}$ | $P_{40}$ | $P_{41-}$ | $P_{42+}$ | $P_{43-}$ | $P_{44+}$ |
|---|---|---|---|---|---|---|---|---|---|---|
| form B | | | | | | | | | | |
| O(2) | −0.013(6) | −0.002(6) | −0.002(6) | 0.006(5) | −0.003(5) | | | | | |
| N(1) | −0.009(6) | 0.104(6) | 0.011(5) | 0.021(5) | −0.010(5) | | | | | |
| N(3) | −0.012(6) | 0.116(6) | −0.014(6) | 0.002(6) | −0.001(6) | | | | | |
| C(2) | −0.019(9) | 0.255(7) | 0.011(7) | −0.014(6) | −0.007(6) | | | | | |
| C(6a) | 0.067(9) | 0.046(10) | | | 0.290(9) | 0.092(13) | 0.012(9) | −0.040(12) | −0.131(12) | −0.001(12) |
| C(3a) | 0.053(10) | 0.051(10) | | | 0.282(10) | 0.086(14) | 0.011(10) | −0.008(12) | −0.099(12) | −0.025(13) |

[a] Atom-based orthonormal frames defined by the following: O(2), Z along O(2) → C(2), Y in {O(2), C(2), N(1)} plane, toward N(1); C(2), Z along C(2) → O(2), Y in {O(2), C(2), N(1)} plane, toward N(1); N(1), Z along N(1) → H(1), Y in {H(1), N(1), C(2)} plane, toward C(2); H(1), Z along H(1) → N(1), Y in {H(1), N(1), C(2)} plane, toward O(2); C(6a), Z along C(6a) → C(3a), Y in {H(6a), C(6a), C(3a)} plane, away from N(1); H(6a), Z along H(6a) → C(6a), Y in {H(6a), C(6a), C(3a)} plane, toward C(3a). Frames for C(3a), H(3a), N(3), and H(3) in form B are constructed in a similar fashion to that for frames for C(6a), H(6a), N(1), and H(1), respectively. All frames are right-handed.

bond length 1.246 Å, average N—C(=O) bond length 1.351 Å, average N—C(C—C) bond length 1.446 Å, and average C—C bond length 1.566 Å. These values compare quite well with those found in *d*-biotin[8] (1.249, 1.341, 1.453, and 1.548 Å, respectively) and in a series of heterobiotin analogs[9] and chainless heterobiotin analogs.[11] Thus in a family of structures in which the ureido moiety participates in maximal hydrogen bonding (each NH donating, each O accepting) the carbonyl C=O bond is lengthened from a standard value (1.21 Å) and the N—C(=O) bonds are shortened from a standard value (1.47 Å). A picture of the electronic structure inferred from the bond lengths alone is one in which two canonical structures are mixed, more or less in equal proportion.

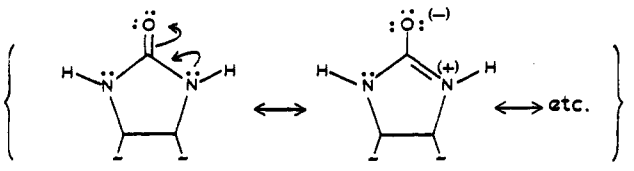


The interdependence of the C=O and C—N bond lengths in ureido ring structures in particular, and in urea structures in general, has been the subject of our investigations, and in terms of their geometry the ureido rings of glycoluril fall within the parameters of this family of structures.[18] There a plot of the C=O versus N—C(=O) bond lengths can be fitted by a line $d$[C=O] (Å) = 3.210 Å − 1.462$d$[N—C(=O)] (Å). Glycoluril in its consensus structure predicts a carbonyl bond length of 1.235 Å, slightly shorter than that observed. This is in part due to a systematic bias in the positioning of a terminal oxygen, such as a carbonyl oxygen, from traditional room temperature, moderate resolution diffraction studies such as those that make up the body of the database of structures that fitted the line.

The ureido rings in both forms are nearly, but not exactly, planar. If planes are fitted to the bond-contiguous atomic positions N–C–C–N, it can be seen, Figure 3, that the ureido rings are slightly bent about an axis through the nitrogen atoms. In form A, with the symmetrical crystalline environment, the carbonyl C=O group folds back the butterfly wings of the *cis*-fused junction; the molecule is extended a bit by such a folding. The NH hydrogen atoms are likewise folded back, on the same side of the least-squares plane as the C=O group. Dreiding models of the molecule built with trigonal nitrogens deform so that a bending of the C=O group below the N–C–C–N plane brings the NH hydrogens above the plane. In the crystal structure of form A the opposite occurs. Similar folding of the ureido ring has recently been demonstrated for a series of chainless heterobiotin molecules studied crystallographically and by *ab initio* quantum chemical methods.[11] In form B the ring planes are nearly exact. There are very minimal deviations of the carbonyl atomic positions from the N–C–C–N planes. The NH hydrogens are, however, more variable. One is above and one below the N–C–C–N plane, and their positions track quite well the oxygen atoms on neighboring molecules to which they hydrogen bond. Given that the crystalline environment for the molecule in form B is unsymmetrical, it is not surprising that the effect of dissymetry

(18) Blessing, R. H. *J. Am. Chem. Soc.* **1983**, *105*, 2776–2783.

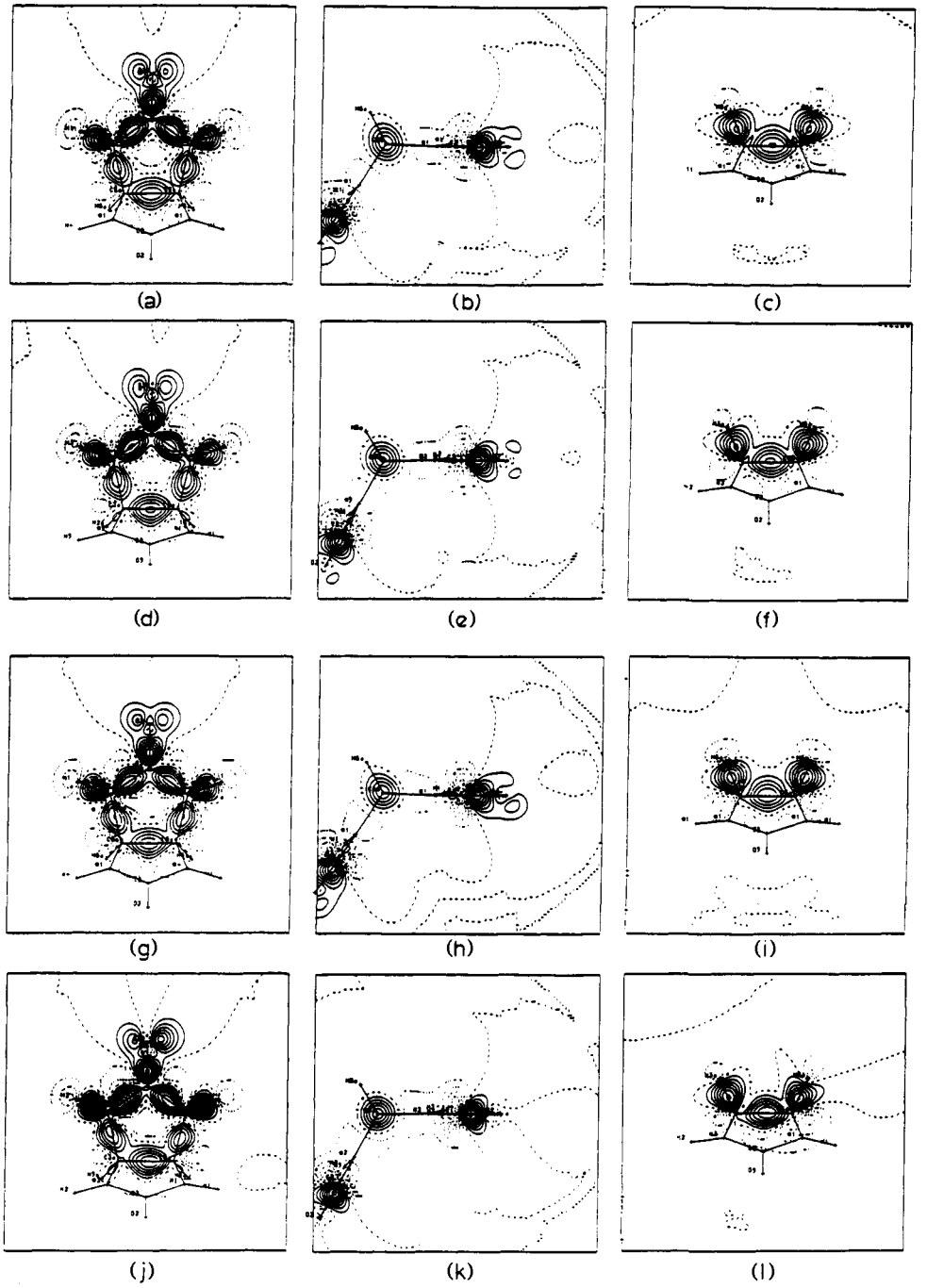


**Figure 4.** Static deformation density maps of glycoluril constructed in direct space: (a–c) form A, 105 K; (d–f) form B, 105 K; (g–i) form A, 293 K; (j–l) form B, 293 K. Sections are described in the text. Contour intervals are 0.1 e/Å$^3$. In principle the effects of thermal motion have been removed from these maps and features within a form should be comparable from temperature to temperature. The only significant difference is in the oxygen atom lone pair region for form B (maps g and j), where an apparent dissymmetry in the density at room temperature is absent at low temperature.

should appear in the placement of the hydrogen-bonded hydrogen atoms. Because form A is about 2% more dense than form B, the molecule in form A might be predicted to flatten a bit to pack more compactly, but our theoretical results (*vide infra*) suggest that the flattening in form A results from the two-dimensional network of hydrogen bonds alone. Packing in the third dimension is not necessary to account for the observed flattening.

**Details of the Hydrogen Bonding.** The hydrogen-bonding pattern in form A is identical to that found in biotin methyl ester[9] and biotin-*d* sulfoxide.[9] Distances from the NH nitrogen donor on one molecule to the C=O oxygen acceptor on another molecule are 2.846 Å at 105 K and 2.860 Å at 293 K. These values are from 0.06 to 0.21 Å shorter than comparable ones found in the biotin analogs. The pattern of hydrogen bonding in form B is more complex, finding a match in the crystal structure of the chainless analog of biotin.[11] The N···O distances on the symmetric side of the molecule are 2.850 Å at 105 K and 2.871 Å at 293 K, while distances on the opposite, dissymetric side of the molecule are 2.828 Å at 105 K and 2.849 Å at 293 K. Again, these values are smaller than comparable ones for the chainless biotin derivative (2.90 and 2.85 Å at 293 K, respectively).

**Static Deformation Density Maps.** Maps of the static deformation density[19] are shown in Figure 4, for both forms at both temperatures, in three principal sections through the molecule. The same sections are used to map the electrostatic potential (*vide infra*). The first section is approximately in the plane of the ureido ring. The origin of the section is defined by the midpoint of the intracyclic N···N line. The cross product of

(19) Coppens, P. In *Electron Distributions and the Chemical Bond*; Coppens, P., Hall, M. B., Eds.; Plenum Press: New York, 1982; pp 61–92.

the vectors from the origin to the nitrogen and oxygen atoms defines the projection axis. The second section is approximately perpendicular to the first. Its origin is the carbonyl carbon atom. The cross product of the two carbonyl carbon–nitrogen vectors and the carbonyl carbon–oxygen vector define the projection plane. The third section is through the bridgehead C–C bond and is approximately perpendicular to the second section (but not to the first). It is defined by the cross product of the carbon–carbon bond and the carbon–hydrogen bridgehead bond. Both hydrogen atoms are in the plane of the third section. Static maps are direct space summations of the deformation density terms that result from the least-squares refinements and are not Fourier syntheses. They are constructed by summing the values of $\rho_j(\vec{r})$ over all of the atoms in the molecule and subtracting core and unperturbed valence contributions for all the atoms. They are not thermally smeared and are thus a good indicator of the success of the deconvolution of thermal effects from charge density effects. In principle, static maps of a crystal form should be similar if thermal effects were successfully deconvoluted at both temperatures. Examination of the direct space mapping suggests that deconvolution was reasonably complete. Deformation features, both positive and negative, are marginally larger in absolute terms at room temperature than at low temperature for both forms, in line with a notion that thermal motion effects were less completely deconvoluted at room temperature. The only significant differences, however, are confined to the oxygen atom lone pair regions.

Deformation density maps have been interpreted as the rearrangement of electron density when a promolecule (a set of spherical, isolated atoms placed at the proper positions for bonding) is allowed to relax and redistribute electron density due to bond formation. Such interpretation is perhaps unwarranted and can occasionally be misleading.[20,21] Nonetheless it is useful to compare the results of rigid pseudoatom refinements across crystal forms and across crystal temperatures. Such a comparison allows an assessment of the effect of the crystalline environment on the electronic charge distribution of a molecule and an assessment of the smearing effect of finite crystal temperatures upon the molecular densities.

The general features of the maps are in excellent agreement. There are positive accumulations of electron density in all of the "bond regions" and additional accumulations in what are nominally "lone pair regions" on the ureido oxygen atoms. The accumulations are higher in the N—C(=O) bonds than in the N—C(—C) bonds. The effect of crystalline environment is seen most apparently in the lone pair region of the oxygen atoms. In form A the deformation density is necessarily bilaterally symmetric so the idealized picture of two lone pairs symmetrically placed about the C–O direction and in the ureido plane is a necessary consequence of crystallographic symmetry. In form B that symmetry is not required. At room temperature the lone pair on the symmetric side of the molecule appears as a marginally higher accumulation of density than the lone pair on the dissymmetric side; this is in part a consequence of mapping the deformation density onto a single plane. The dissymetry is much less apparent at low temperature, indicating that thermal deconvolution about the terminal oxygen atom at room temperature is likely incomplete. Dissymetry in the deformation density is small in the ureido oxygen atom lone pair region and hardly extends beyond there. The N—C(=O) and N–C(–C) bond regions on the symmetric and dissymetric sides of the molecule in form B are respectively equivalent, and the C—C bond region is the same from form to form. Even though the environment of the molecule in the two crystalline forms is quite different, the molecular charge density appears to be transferable at the quantitative level.

(20) Kunze, K. L.; Hall, M. B. *J. Am. Chem. Soc.* **1986**, *108*, 5122–5127.
(21) Dunitz, J. D.; Schomaker, V.; Trueblood, K. N. *J. Phys. Chem.* **1988**, *92*, 856–867.

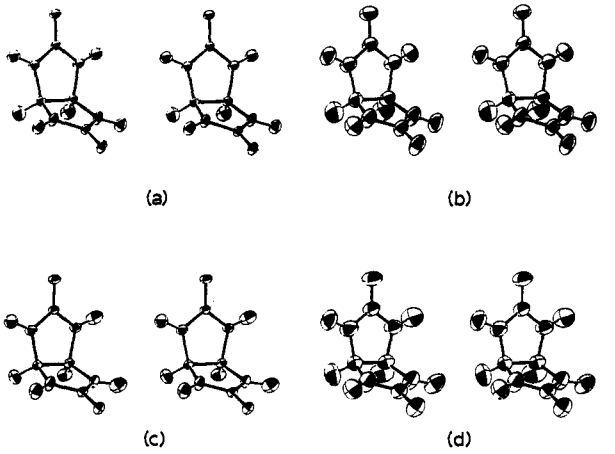


**Figure 5.** Stereo ORTEP diagrams of glycoluril in both crystalline forms at both temperatures. ADPs for the room temperature experiments are from the pseudomultipole refinements. Probability ellipsoids are at the 70% level: (a) form A, 105 K; (b) form A, 293 K; (c) form B, 105 K; (d) form B, 293 K.

**Anharmonic Thermal Motion.** In addition to the harmonic, anisotropic ADPs modeled for all atoms, additional terms that allow for anharmonic, anisotropic ADPs in a Gram–Charlier expansion[22] about the harmonic terms are present for the nitrogen and oxygen atoms. Their necessity was indicated in an examination of early difference density maps that showed strong, chemically unreasonable, dipolar features about those atoms, in directions where anharmonic motions could be expected. Their presence was validated both by the appearance of subsequent maps (an admittedly subjective criterion) and by the significant improvement in agreement between observed and calculated structure factor amplitudes. Neither the bridgehead nor the carbonyl carbon atoms required an elaboration of the ADP model to include anharmonicity.

Subsequent to the full multipole refinements using the low-temperature data, an additional set of refinements of the room temperature data for both crystal forms, fixing multipole parameters at the values determined in the corresponding low-temperature refinements, were undertaken. A scale factor, positional parameters for non-hydrogen atoms, and anisotropic, harmonic and anharmonic ADPs were varied, while hydrogen atom positions were fixed by standard bond lengths and their ADPs by the previous multipole refinements. A total of 44 parameters were varied for form A and 79 parameters were varied for form B. Agreement indices were $R_w = 0.031$ for form A and $R_w = 0.034$ for form B. In subsequent analyses of the ADPs we refer specifically to those determined from these "pseudomultipole" refinements for the 293 K data and to the full multipole refinements for the 105 K data, Figure 5. The pseudomultipole ADPs are given in Table 6.

Anharmonic terms for the nitrogen and oxygen atoms are significant at both temperatures and in both crystal forms, although at 105 K their values are approximately 20–30% of their values at 293 K. The anharmonic terms die out more quickly than their harmonic counterparts, which at low temperature are about 40% of their room temperature values. The reduction is much more varied for the anharmonic terms; some become insignificantly different from 0 at 105 K while others are as much as 40% of their room temperature values at low temperature. In contrast, the reduction in the harmonic, anisotropic ADPs on going from 293 to 105 K is much more uniform; the average ratio of $U_{ij}^{105\text{ K}}/U_{ij}^{293\text{ K}}$ for form A is 0.407 and for form B is 0.403. The ratio of the temperatures, (105 K)/(293 K), is 0.36. Were the low-temperature experiments conducted above the Debye temperatures, where $\Delta U/\Delta T$ is expected to be linear, the average

(22) Zucker, V. H.; Schulz, H. *Acta Crystallogr.* **1982**, *A38*, 563–568.

Table 6. Coordinates, ADPs, and Third-Order Anharmonic Parameters from Pseudomultipole Refinement of 293 K Data

a. Coordinates

| | x/a | y/b | z/c | | x/a | y/b | z/c |
|---|---|---|---|---|---|---|---|
| form A | | | | | | | |
| O(2) | 0 | 0.775 84(5) | 0.533 22(3) | C(6a) | 0.105 97(2) | 0.554 74(2) | 0.25 |
| N(1) | 0.149 38(4) | 0.649 16(5) | 0.364 58(3) | H(1) | 0.275 14 | 0.661 47 | 0.399 76 |
| C(2) | 0 | 0.698 25(2) | 0.429 73(1) | H(6a) | 0.164 69 | 0.422 03 | 0.25 |
| form B | | | | | | | |
| O(2) | 0.631 23(3) | −0.040 35(4) | 0.329 60(10) | C(3a) | 0.618 25(4) | 0.25 | −0.073 78(10) |
| N(1) | 0.515 34(4) | 0.130 63(5) | 0.250 61(14) | H(1) | 0.458 00 | 0.099 52 | 0.389 47 |
| N(3) | 0.668 16(4) | 0.130 67(5) | 0.024 82(15) | H(3) | 0.737 27 | 0.094 04 | −0.050 01 |
| C(2) | 0.607 13(2) | 0.064 64(3) | 0.211 37(7) | H(6a) | 0.439 00 | 0.25 | −0.055 79 |
| C(6a) | 0.509 62(3) | 0.25 | 0.085 05(10) | H(3a) | 0.612 21 | 0.25 | −0.316 60 |

b. Anisotropic, Harmonic, Mean-Square Displacement Parameters[a]

| | $U^{11}$ | $U^{22}$ | $U^{33}$ | $U^{12}$ | $U^{13}$ | $U^{23}$ |
|---|---|---|---|---|---|---|
| form A | | | | | | |
| O(2) | 0.022 35(10) | 0.061 54(18) | 0.025 64(11) | 0 | 0 | −0.013 65(12) |
| N(1) | 0.016 93(6) | 0.059 63(14) | 0.024 12(8) | 0.001 69(8) | −0.000 89(6) | −0.009 53(8) |
| C(2) | 0.018 05(9) | 0.041 66(16) | 0.019 71(11) | 0 | 0 | −0.003 22(11) |
| C(6a) | 0.021 32(10) | 0.034 86(14) | 0.020 22(10) | 0.004 33(11) | 0 | 0 |
| H(1) | 0.020 67 | 0.048 10 | 0.036 74 | −0.001 99 | −0.007 67 | −0.001 35 |
| H(6a) | 0.041 27 | 0.058 77 | 0.044 24 | 0.010 15 | 0 | 0 |
| form B | | | | | | |
| O(2) | 0.028 78(10) | 0.028 03(12) | 0.047 65(15) | 0.005 53(8) | 0.000 64(10) | 0.009 88(11) |
| N(1) | 0.025 26(11) | 0.026 27(12) | 0.044 08(15) | 0.004 21(9) | 0.006 64(10) | 0.008 72(12) |
| N(3) | 0.034 32(14) | 0.030 28(14) | 0.052 93(19) | 0.008 70(12) | 0.017 99(13) | 0.009 63(14) |
| C(2) | 0.023 47(11) | 0.022 19(12) | 0.033 11(14) | 0.002 14(10) | 0.000 43(10) | 0.002 02(11) |
| C(6a) | 0.023 71(17) | 0.021 00(16) | 0.031 25(10) | 0 | −0.003 62(15) | 0 |
| C(3a) | 0.033 81(21) | 0.024 15(18) | 0.026 05(19) | 0 | 0.003 61(16) | 0 |
| H(1) | 0.023 73 | 0.038 53 | 0.064 55 | −0.005 06 | 0.004 71 | 0.004 43 |
| H(3) | 0.032 95 | 0.042 49 | 0.051 03 | 0.007 03 | 0.016 15 | −0.005 04 |
| H(6a) | 0.046 57 | 0.042 30 | 0.056 12 | 0 | −0.019 83 | 0 |
| H(3a) | 0.045 10 | 0.059 48 | 0.036 51 | 0 | 0.015 14 | 0 |

c. Third-Order Anharmonic Parameters (×10³)

| | | form A | form B | | form A | form B |
|---|---|---|---|---|---|---|
| O(2) | C111 | | −0.13(6) | C113 | −0.10(3) | −0.14(5) |
| | C222 | 0.39(15) | 0.42(7) | C133 | | 0.43(6) |
| | C333 | −0.50(6) | 0.55(12) | C223 | −0.66(7) | 0.56(5) |
| | C112 | 0.08(4) | 0.07(4) | C233 | 0.68(5) | 0.75(6) |
| | C122 | | 0.19(4) | C123 | | 0.23(4) |
| N1 | C111 | 0.04(3) | 0.16(6) | C113 | 0.01(2) | 0.37(5) |
| | C222 | −0.04(11) | 0.12(7) | C133 | −0.10(2) | 0.31(6) |
| | C333 | −0.07(4) | 0.04(12) | C223 | 0.22(5) | 0.21(5) |
| | C112 | −0.13(3) | 0.20(4) | C233 | 0.01(3) | −0.03(7) |
| | C122 | −0.46(4) | 0.14(4) | C123 | 0.26(3) | 0.22(4) |
| N3 | C111 | | −0.21(9) | C113 | | −0.23(7) |
| | C222 | | 0.13(8) | C133 | | 0.16(8) |
| | C333 | | 0.41(15) | C223 | | 0.29(7) |
| | C112 | | −0.09(6) | C233 | | 0.50(8) |
| | C122 | | 0.31(5) | C123 | | 0.08(5) |

[a] See footnotes to Table 4.

ratios $U_{ij}^{105\ K}/U_{ij}^{293\ K}$ would equal 0.36. The fact that they do not suggests that the low-temperature experiments were conducted below the Debye temperatures. These crystals, which decompose without melting at ~615 K for both forms, are very hard, and a Debye temperature greater than 100 K is not unreasonable.

Rigid bond tests[23] on the mean square displacement amplitudes (Å²) along bond directions for bonded non-hydrogen atoms suggest that the deconvolution of charge density parameters and ADPs at low temperature is satisfactory. The largest value of $\Delta U^2$ along bonds at 105 K is 0.0003 Å² for form A and 0.0004 Å² for form B. The rigid bond criterion is a necessary, but not sufficient, criterion of the completeness of the deconvolution. With the multipole model fixed in the pseudomultipole refinements of the 293 K data, the rigid bond test indicates a reasonable deconvolution, with maximum values of $\Delta U^2$ along bonds of 0.0004 and 0.0003 Å² for form A and form B, respectively.

**Rigid Body Analysis of the ADPs.** The modes of thermal motion for both crystal forms, at both experimental temperatures, were analyzed in terms of a rigid body model.[21] In a first model, model I, the ADPs of the non-hydrogen atoms were fitted to rigidly translating and librating bodies for each form. The resultant fits between "observed" ADPs and calculated temperature factors were only modestly satisfactory for all the experiments. The models were elaborated in a number of ways to include, in addition to rigid body motion, nonrigid, internal motions of various subgroups of the molecule. The most sensible and best fitting elaboration allowed for nonrigid motion of the nitrogen and oxygen atoms. There were the same atoms for which anharmonic terms in the ADPs were necessary in the refinements. The nitrogen atom nonrigid motions were treated as secondary librations about the O=C axes while the nonrigid motions of the oxygen atoms were treated as secondary librations about the brigehead C—C axes, model II. The results of fits for both temperatures and both crystal forms are detailed in Table 7. The agreement is very good in every case. A simplified mechanical interpretation of model II has the urea functionality –HN–CO–NH– maintaining planarity while the bicyclic ring flexes about

(23) Hirschfeld, F. L. *Acta Crystallogr.* **1976**, *A32*, 239–242.

Table 7. Goodness-of-Fit Indices and Root-Mean-Square Principal Amplitudes for Rigid-Body Translations (T) and Librations (L) and for Nonrigid Translations[a]

| | | form A | | | | form B | | | |
|---|---|---|---|---|---|---|---|---|---|
| | | 105 K | | 293 K | | 105 K | | 293 K | |
| | | model I | model II | model I | model II | model I | model II | model I | model II |
| $R_w$ | | 0.1987 | 0.0145 | 0.1508 | 0.0135 | 0.2161 | 0.0324 | 0.1622 | 0.0269 |
| $S$ | | 88.2 | 7.14 | 44.7 | 4.45 | 44.0 | 7.16 | 34.9 | 6.28 |
| $N_o$ | | 28 | 28 | 28 | 28 | 32 | 32 | 32 | 32 |
| $N_p$ | | 12 | 15 | 12 | 15 | 12 | 15 | 12 | 15 |
| $(u^2)^{1/2}$ (Å) | $T_1$ | 0.121(11) | 0.1103(10) | 0.188(12) | 0.1778(14) | 0.11(2) | 0.101(3) | 0.17(2) | 0.161(3) |
| | $T_2$ | 0.099(5) | 0.0896(5) | 0.151(6) | 0.1393(8) | 0.102(5) | 0.094(1) | 0.158(6) | 0.148(1) |
| | $T_3$ | 0.081(9) | 0.0822(7) | 0.126(9) | 0.1265(9) | 0.091(2) | 0.092(1) | 0.146(4) | 0.146(1) |
| $(\omega^2)^{1/2}$ (deg) | $L_1$ | 3.8(9) | 2.78(11) | 5.8(1.1) | 4.37(15) | 4.3(9) | 3.1(2) | 7(1) | 4.7(3) |
| | $L_2$ | 1.6(5) | 1.85(7) | 3.0(5) | 2.98(10) | 1.3(4) | 1.56(8) | 2.4(4) | 2.5(2) |
| | $L_3$ | 0(4) | 0.68(10) | 1(2) | 1.19(11) | 0(2) | 0.83(2) | 1(2) | 1.4(2) |
| lib group and torsion angle: $(\omega^2)^{1/2}$ (deg) | | N(1) | 5.45(8) | | 7.6(1) | | 5.2(2) | | 7.0(3) |
| | | N(3) | 5.45(8) | | 7.6(1) | | 6.9(2) | | 9.0(2) |
| | | O(2) | 0.89(11) | | 1.5(1) | | 0.6(3) | | 1.5(3) |
| displacement: $(u^2)^{1/2}$ (Å) | | N(1) | 0.1051(15) | | 0.146(2) | | 0.100(3) | | 0.136(4) |
| | | N(3) | 0.1051(15) | | 0.146(2) | | 0.132(3) | | 0.172(4) |
| | | O(2) | 0.053(7) | | 0.09(1) | | 0.04(3) | | 0.09(2) |

[a] Model I, rigid molecule; model II, rigid molecule plus nonrigid vibrations of N and O atoms. $R_w = [\sum w\Delta^2(U^{ik})/\sum w(U^{ik})^2]^{1/2}$, $w = 1/\sigma^2(U^{ik})$. $S = [\sum w\Delta^2(U^{ik})/(N_o - N_p)]^{1/2}$. $N_o$ = number of independent-atom $U^{ik}$ values. $N_p$ = number of parameters of the TLS plus nonrigid group librations. The largest value of the $S$ tensor for all model II fits is 0.12(2) deg·Å.

the bridgehead C–C bond. As the intra-ring N–C–C–N torsion angle departs from 0, the nitrogens on opposite sides of each ring flex antisymmetrically. The oxygen atoms, which are rigidly tied to the urea functionalities, move in a direction roughly perpendicular to the ring plane. According to the model the out-of-plane motions of the nitrogen atoms should be larger than those of the oxygen atoms, and the carbon atoms remain fixed in the rigid body. An alternate scenario, in which there are C=O bending motions out of the N–C–C–N plane, does not fit the rigid body model nearly as well as the one just described.

Looking at the fits of model II to the ADPs of both crystal forms it is clear that, in spite of differences in crystalline environment, the rigid body motions of the glycoluril molecule are transferable at a given crystal temperature. The largest translational motions are those perpendicular to the mean plane of the molecule, but they are not much larger than the other two components. The largest librations are about the major inertial axis (parallel to the O···O vector and intersecting the ureido rings) of the molecule; the smallest are about the minor inertial axis, perpendicular to the mean plane of the molecule. Interpreted in terms of their respective crystal structures and environments, Figures 1 and 2, these motions are just those that maximally preserve hydrogen bond contacts. Looking from room temperature to low temperature it is clear that thermal translational and librational motions are greatly reduced, and nonrigid motions are diminished but still significant, paralleling the behavior of the anharmonic ADPs for those atoms.

The correlation of rigid body motion with thermal expansion is rather good for form A. In that form both the largest rigid body translations and rigid body librations are such as to move atoms in all molecules parallel to the crystallographic *b*-axis. Rectilinear translational motion is essentially harmonic and thus cannot affect the unit cell dimensions, but libratory motion has an anharmonic component that can manifest itself in thermal expansion. The crystallographic *b*-axis expands ~2.2% upon raising the crystal temperature; virtually all of the volume change with warming is due to the change in $|b|$. That axis is perpendicular to the main plane through the molecule (a plane parallel to the one containing all four nitrogen atoms). For form B the situation is more complicated. There the approximately perpendicular arrangement of molecules in the crystal structures, with no single direction in the crystal parallel or perpendicular to the main directions in all the glycoluril molecules, suggests that all of the lattice dimensions should respond by expansion upon warming to a more or less equal degree, which they do.

***Ab Initio* Quantum Chemical Studies of Glycoluril.** *Ab initio* calculations were carried out on glycouril both as the isolated molecule and as the central molecule in a pentameric fragment lifted from the form A crystal structure. Calculations for the isolated molecule and for the central molecule of the cluster were carried out in a 6-31G** basis, while in the pentamer calculations the neighboring four glycoluril molecules were modeled in a smaller basis (3-21G). Initial calculations, for the purpose of comparing electronic features, were done by fixing the nuclear geometry at the experimental position from the 105 K refinements of form A. Subsequently, to test the responsiveness of the ureido ring geometry to its environment, the nuclear geometries of the monomer and pentamer were allowed to relax. Analytic first derivatives of the total energy with respect to the nuclear coordinates were used to locate a minimum on the potential energy surface of the pentamer. All calculations were carried out using HONDO-8[24] on an IBM RS/6000 workstation. Maps were constructed from the wave functions using the KGNGRAF package.[25]

From the standpoint of the theoretical static deformation density, Figure 6, the results of the pentamer calculation and the isolated molecule calculation are qualitatively similar. It should be noted that Figure 6a shows the total pentamer density minus the spherical atom contribution of the *central* promolecule only, making the density at the periphery very high. The principal sections shown are the same as for the experimental work. Quantitatively the total density of the isolated monomer (frozen at the pentamer geometry) can be subtracted from the total density of the pentamer and the redistribution of charge density upon incorporation of the monomer into the experimentally observed hydrogen-bonding environment can be mapped. Maps g and h of Figure 6 show such difference maps for glycoluril in two of the three principal sections (there were no contours above the 0.02 e/Å$^3$ level for the third projection). Note that the contour interval for this difference mapping is much smaller than the total-minus-spherical atom density mapping. The theoretically predicted charge density redistribution upon incorporation into the pentamer parallels the results on urea where the calculations were performed

(24) (a) Dupuis, M.; Maluendes, S. A. In *Modern Techniques in Computational Chemistry*; Clementi, E., Ed.; ESCOM: Leiden, 1991. (b) Dupuis, M.; Chin, S.; Marquez, A.; *CHEM-Station and HONDO in Relativistic and Electron Correlation Effects in Molecules and Clusters*; Malli, C. L., Ed.; Plenum Press: New York, 1992.

(25) Chin, S.; Martins-Costa, M.; Tagliavini, R.; Rondeau, S. B.; Prost, J. P. In *Modern Techniques in Computational Chemistry (MOTECC-91)*; IBM Corporation: New York, 1989.

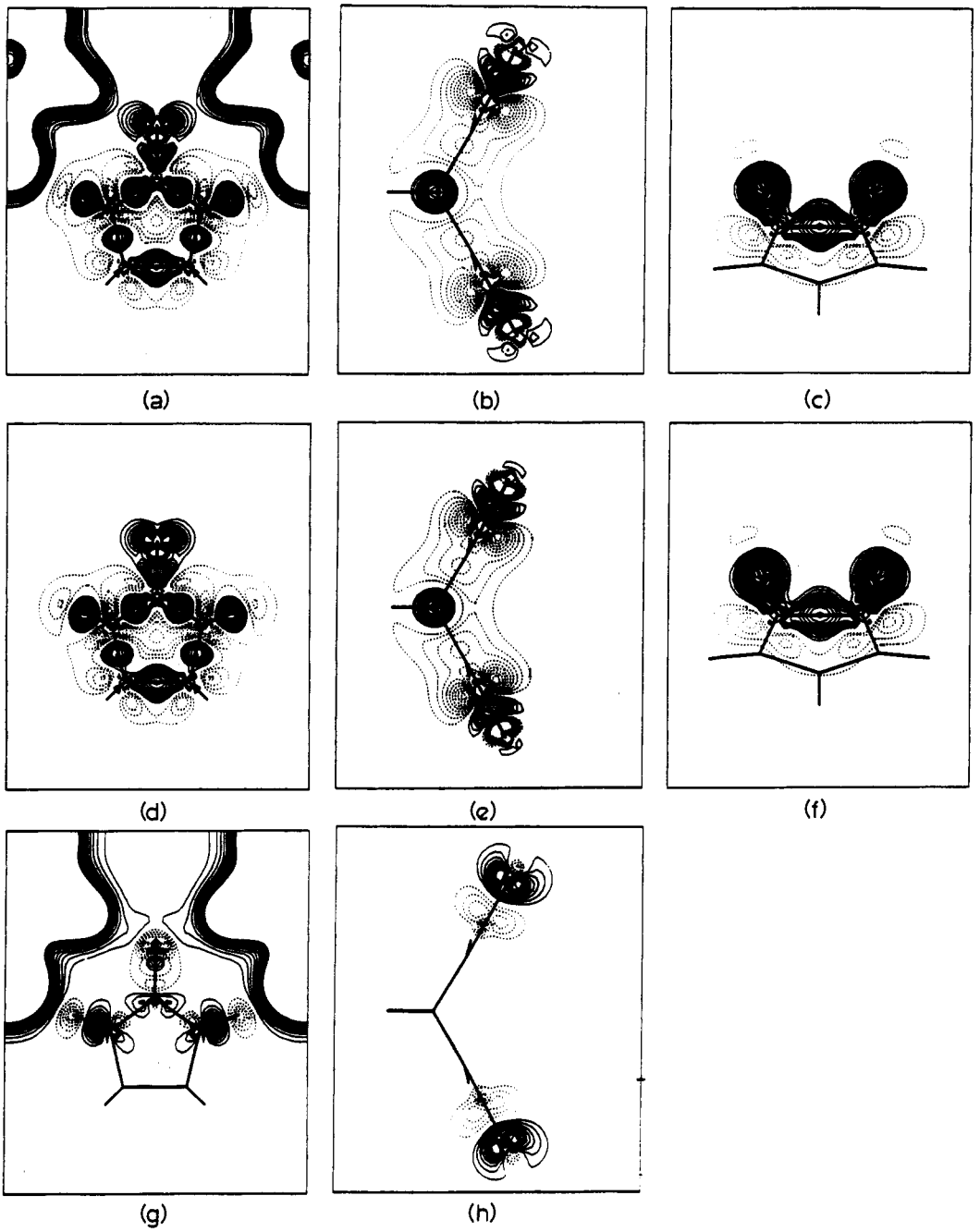


**Figure 6.** Static deformation density maps of glycoluril from the theoretical calculations. Principal sections are as in Figure 4, described in text. At the top (a–c) are the results of the pentamer calculations with the total density minus the spherical atom contributions of the central molecule. In map a the large accumulations to the left and right of the central molecule are the *total* densities of the hydrogen-bonded neighbors. In the middle row (d-f) are the results from the isolated monomer frozen at the geometry of the pentameric structure. On the bottom (g, h) are the differences between the top and middle row maps; i.e., map g is calculated by subtracting map d from map a. Contour intervals for maps a-f are 0.05 e/Å$^3$; for maps g and h, 0.02 e/Å$^3$. The map corresponding to map c minus map f is not shown because there were no contours at the 0.02 e/Å$^3$ level. The central molecules in both the pentamer and monomer calculations were described by 6-31G** basis sets; the peripheral molecules in the pentamer were described in a 3-21G basis set. These maps are, in principle, directly comparable with those from the static mapping of the experimentally determined multipole parameters, Figure 4.

in the 6-21G** basis using the Hartree–Fock LCAO program CRYSTAL for periodic systems.[26] In both the glycoluril and the urea calculations, incorporation of an isolated molecule into its hydrogen-bonded environment, modeled in the former by the nearest neighbors in a small basis or in the latter by the infinite crystal lattice in an elaborated basis, redistributes charge density from the periphery to the interior of the molecule. Dovesi *et al.*[26] attribute the redistribution to intermolecular exchange forces which cause a contraction of the electronic cloud attending crystal formation. Whereas, in urea, it can be said that all of its atoms constitute the molecular periphery, in glycoluril the bridgehead carbon atoms and their hydrogens might be considered as occupying the molecular interior. There are no discernible rearrangements of charge density predicted by the pentamer calculations for the bridgehead C–C or C–H bond regions. The largest shifts upon incorporation in the crystal lattice for urea are in the regions associated with the lone pairs on the carbonyl oxygen atom. The same is true for glycoluril in the pentamer.

A comparison of the static maps constructed from the multipole parameters of the 105 K refinement results for form A, Figure 4a–c, with the theoretical results, Figure 6a–c, indicates overall qualitative agreement as to the shape and placement of features.

(26) Dovesi, R.; Causa, M.; Orlando, R.; Roetti, C.; Saunders, V. R. *J. Chem. Phys.* **1990**, *92*, 7402–7411.

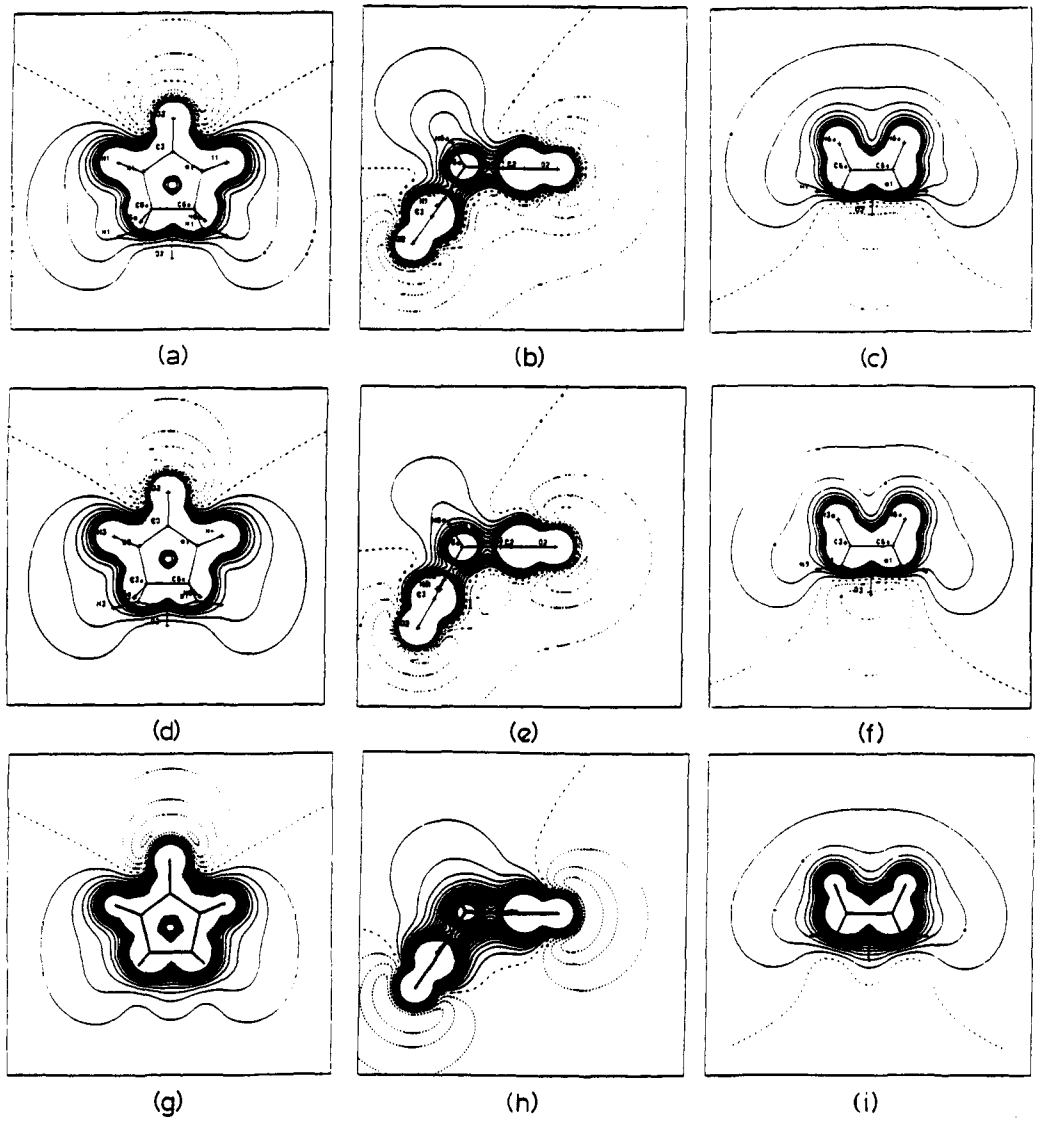


**Figure 7.** Maps of $\phi(\bar{r})$, the electrostatic potential, of glycoluril from experiment and theory. Only the low-temperature maps from experiment are shown. Principal sections are as in Figure 4, described in text. Maps a-c are from form A, d-f from form B, and g-i from the isolated monomer calculation. Contour intervals are 0.05 e/Å. Since the theoretical potential was calculated directly from the wave function, it was necessary to resort to the monomer calculation for comparison. The most negative values of the potential (–0.2 e/Å) are found in the inside pocket of the molecule formed by the *cis*-fused rings, close to the ureido oxygens.

Thus about the carbonyl carbon atom there are trigonally disposed maxima of $\Delta\rho$ along all the bond paths. All three maxima are closer to the carbonyl carbon position than to the atoms along the bond paths (oxygen and the two nitrogen atoms). Likewise, above and below the carbonyl carbon position in the ureido plane there are symmetrically disposed deep minima close by. The maxima associated with the carbonyl oxygen lone pair directions are clearly evident in both theory and experiment, and even the bowing of the C–C density outside the ureido ring–ring junction is apparent in both. The chemically different N—C bonds are clearly distinguished by the maxima in their bond directions; the conjugated N—C(=O) bond shows more difference density than the N—C(—C) bonds in both experiment and theory. In quantitative terms the comparisons are very acceptable. Looking at the regions at the midpoints of chemical bonds, the differences between experiment and theory are no greater than 0.1 e/Å$^3$ (note that the experimental static deformation maps are contoured on an interval of 0.1 e/Å$^3$ while the theoretical maps are contoured on an interval of 0.05 e/Å$^3$). Likewise, the holes behind the carbonyl carbon atom are as deep, with a difference less than 0.1 e/Å$^3$. The largest differences are found in the carbonyl oxygen lone pair regions. There the deformation density in the theoretical map is 0.3 e/Å$^3$ larger than the corresponding region in the experimental map. The shifts found in that same region in the theoretical maps going from an isolated monomer to a pentamer are in the direction of reducing the deformation density in the lone pairs, and it is reasonable to speculate that were the peripheral molecules of the pentamer modeled in a more extended basis, the difference between theory and experiment would be further reduced.

The agreement between geometrical measures of the glycoluril molecule could scarcely be improved. The results of the geometry optimizations both on the isolated monomer and on the central molecule of the pentamer are shown with the experimental values in Figure 3. Clearly the ureido ring responds significantly to its crystalline environment. The carbonyl C=O bond length in the pentamer is 0.03 Å larger than the corresponding length in the monomer (1.231 *versus* 1.197 Å, respectively) while the N—C(=O) bond lengths are shorter by 0.02 Å (1.344 *versus* 1.367 Å, respectively), to make the agreement with experiment (C=O, 1.246 Å; N—C(=O), 1.351 Å) much better. The N–C–N bond angle, which opens from 106.4° in the monomer to 109.3° in the pentamer, is now in accord with experimental results, 109.3°. The agreement extends to the hydrogen atom results. In the experimental refinements the C–H and N–H bond *lengths*, but not their directions, were fixed at standard values, yet the C–N–H

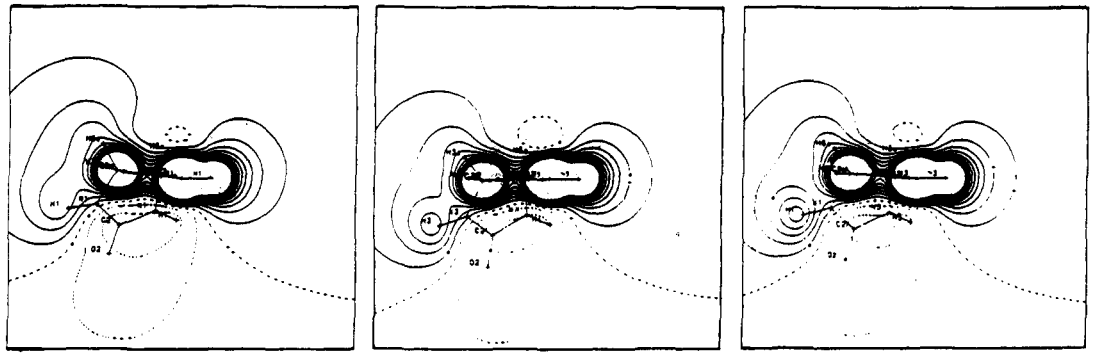


**Figure 8.** The electrostatic potential of glycoluril above and below the ureido nitrogen atoms as determined experimentally. The sections are constructed with the nitrogen atoms as origin, the N–H vectors defining the horizontal axes, and the cross products between the two N–C bonds defining the planes (in the figures these cross products are approximately vertical). Map a is for form A, 105 K. Maps b and c are for the two independent nitrogen atoms of form B, 105 K. There are small zero contour level features appearing just above the nitrogen atoms while modestly negative values of $\phi$ below the nitrogen atoms are part of the basin of negative potential filling the inner pocket of the molecule.

angles, for example, are essentially identical in the experimental results and the results from the pentamer calculations. The displacements of the carbonyl oxygen and carbon atoms and the NH hydrogen atoms from planes fitted to the bond-contiguous atomic positions N–C–C–N show that the monomer, which is folded in slightly, opens a bit to extend itself in the pentamer structure, just as observed experimentally. Again the hydrogen atoms and the carbonyl oxygen and carbon atoms are on the same side of the N–C–C–N plane, as observed experimentally, although the deviations as calculated are not as pronounced as observed. It seems that every feature of the geometry of the molecule is in good agreement as soon as a part of the crystalline environment is incorporated into the calculations.

**The Molecular Electrostatic Potential.** Unlike the deformation density, which is an artificial construct that makes use of an arbitrary, albeit sensible, reference state, the electrostatic potential is an observable of the system in the sense that, in principle, an experiment can be devised to measure it directly at every point about the molecule. Its importance in molecular interactions is clear. Stewart and Craven[27] have recently described the details of the method Stewart[28] described in general outline some years ago to use the experimentally derived multipole parameters to calculate the electrostatic potential of a molecule lifted out of the crystal lattice. Maps of the electrostatic potential of glycoluril in the three principal sections are shown in Figure 7; additional maps of the potential above and below the ureido NH groups are shown in Figure 8.

Given that the deformation densities of the two crystal forms are in qualitative and quantitative agreement, it should come as no surprise that the electrostatic potential for glycoluril in the two forms is very similar. The placement of the zero contours of $\phi(\bar{r})$ and the shape and height or depth of the constant potential contours agree quantitatively. The electrostatic potential clearly differentiates the inner pocket of the molecule, where the potential is everywhere negative, from the back side of the molecule, where it is everywhere positive. This is in contrast to the deformation density, which, being a local feature, suggests that both sides of each ureido ring are equivalent. The arc of negative potential stretching from one oxygen atom to the other has a minimum value about 50° off the C=O bond direction, toward the inside pocket. The inner pocket then would be a site favorable to protonation or electrophilic attachment. The potential directly above and below the nitrogen atoms of the ureido groups is also marginally negative as well, Figure 8, indicating a site of potential protonation; but in line with aqueous solution measurements of amides in dilute acids,[29] the electrostatic potential suggests that O-protonation should be greatly favored over N-protonation.

Urea has been the subject of extensive investigation by Swaminathan *et al.*[30] and by Stewart,[31] who mapped the experimentally determined electrostatic potential of the molecule lifted from the crystal lattice. Qualitatively the potentials in the ureido plane of glycoluril and the molecular plane of urea are very similar, but the potential of the negative region about the oxygen atom of urea is much deeper, –0.35 e/Å, than found for glycoluril, –0.20 e/Å. This correlates well with the decreased basicity of the ureido group *versus* the urea group when the former is incorporated into a five-membered ring.[32] Thus, the $pK_a$ of desthiobiotin is –0.97 while that of 1,3-dimethylurea is –0.20. One needs to be a bit circumspect in drawing conclusions about solution behavior from crystal-extracted electrostatic potentials, since the latter indirectly incorporate the effects of the crystal lattice into the "extracted" molecule; but given that glycoluril and urea can interact through hydrogen bonding with water in the solution studies, much as they do with neighbors in their respective crystal lattices, it seems reasonable to correlate the two properties.

The theoretically derived electrostatic potential of the isolated glycoluril molecule is also shown in Figure 7. In this case it was necessary to forego the calculation of the potential of the molecule in the pentamer since the calculation of $\phi(r)$ was through the wave function rather than through analytical functions fitted to the density. Still, the comparison of the experiment with theory is reasonable. The arc of continuously negative potential connecting the oxygen atoms observed experimentally is not found in the theoretically modeled monomer; but the minima in the plane of the ureido rings are of comparable depth, and the zero potential contours surrounding the nitrogen and bridgehead carbon atoms are superimposable. The positive potential maxima close to the nuclear positions are uniformly higher than those modeled through the diffraction results; these are, however, regions where the experimental results are somewhat less accurate due to the limited extent of the diffraction resolution.

## Discussion

Our studies suggest that a consensus picture of glycouril can be reached, for geometric and electronic properties, so long as adequate deconvolution of thermal smearing effects is achieved

(27) Stewart, R. F.; Craven, B. M. *Biophys. J.*, in press.
(28) Stewart, R. F. *Chem. Phys. Lett.* **1979**, *65*, 355–342; *God. Jugosl. cent. kristalogr.* **1982**, *17*, 1–24.
(29) Martin, R. B. *J. Chem. Soc., Chem. Commun.* **1972**, 793–794.
(30) Swarminathan, S.; Craven, B. M.; Spackman, M. A.; Stewart, R. F. *Acta Crystallogr.* **1984**, *B40*, 398–404.
(31) Stewart, R. F. In *The Application of Charge Density Research to Chemistry and Drug Design*; Jeffrey, G. A., Piniella, J. F., Eds.; Plenum Press: New York, 1991; pp 63–101.
(32) Caplow, M. *Biochemistry* **1969**, *8*, 2656–2658.

in the experimental high resolution diffraction studies and so long as environmental effects are incorporated in the theoretical *ab initio* calculations. Inadequacies in either, or both, are likely the prime cause of what remaining lack of quantitative agreement there is. The transferability of electronic and geometric features, from one crystal environment to another and from one temperature to another (and over the half-dozen crystals used for the diffraction experiments), is rather remarkable. The sensitivity of the theoretical calculations to the molecular environment is equally remarkable. The two methodologies clearly support one another well.

As a model for biotin, glycoluril possesses the requisite *cis*-fused bicyclic ring structure and ureido ring functionality, but lacks the tetrahydrothiophene group found in *endo* geometry in the native coenzyme. Geometically the glycoluril ureido groups fit the pattern of C=O bond elongation and N—C(=O) bond shortening found in biotin itself and in the family of ureido and urea structures analyzed by Blessing.[18] Given the excellent transferability of the charge density at the level of static deformation maps seen in this study, it may not be surprising to predict that, at a local level, the charge density of the ureido group in biotin will be modeled quantitatively by that found here in glycoluril. What remains to be seen is if the electrostatic potential, a property sensitive to the total molecular charge distribution, is appreciably altered when the ureido ring is incorporated into the biotin bicyclic moiety.

**Acknowledgment.** This work was supported in part by NIH Grants DK19856 and GM34073. We thank Prof. Harry King for many helpful discussions concerning the quantum chemical aspects of this work, Prof. Philip Coppens for making MOLLY available to us, and Prof. Claude Lecomte and Dr. Noureddine Ghermani for making the electrostatic potential codes, modified from ones written by Prof. Bryan Craven and Dr. Hans Peter Weber, available to us. We thank our colleague Dr. Mohamed Souhassou for many stimulating discussions.

**Supplementary Material Available:** Final difference Fourier syntheses after multipole refinements of glycoluril forms A and B at low and room temperatures, deformations of the ureido rings of form A from planarity at low temperature, local axial frames employed in the multipole refinements, dynamic deformation density maps of forms A and B at low and room temperatures, and experimental details (5 pages); listing of observed and calculated structure factors for glycoluril forms A and B at low and room temperatures (72 pages). This material is contained in many libraries on microfiche, immediately follows this article in the microfilm version of the journal, and can be ordered from the ACS; see any current masthead page for ordering information.